COMPUTATIONAL
AND STRUCTURAL
BIOTECHNOLOGY
JOURNAL

Celastrol inhibits the proliferation and migration of MCF-7 cells through the leptin-triggered PI3K/AKT pathway

Pingping Chen [a,c], Bin Wang [c], Meng Li [a], Chunxue Cui [a], Fei Liu [a,b,*], Yonggang Gao [a,*]

[a] Hebei University of Chinese Medicine, Shijiazhuang, Hebei 050200, China
[b] Hebei Key Laboratory of Traditional Chinese Medicine Health Care, Shijiazhuang, Hebei 050200, China
[c] The First Affiliated Hospital of Hebei University of Chinese Medicine, Shijiazhuang, Hebei 050017, China

ARTICLE INFO

ABSTRACT

Leptin is the pivotal modulator in the onset and progression of breast cancer and obesity. Celastrol, which is extracted from the roots of Tripterygium wilfordi plants, exerts various anticancer bioactivities and has recently emerged as a candidate to treat obesity by improving leptin sensitivity. However, the relationship between leptin and celastrol in the treatment of breast cancer is unknown. Here, the growth and migration of MCF-7 cells induced by leptin were tested to demonstrate the antineoplastic activity of celastrol. Transcriptomic analysis and western blotting were conducted to explore the biological roles of leptin in treating breast cancer with celastrol. The present findings showed that celastrol remarkably reversed leptin-triggered cell proliferation and migration in MCF-7 cells. Fifty-two mRNAs with fivefold higher counts and 149 mRNAs with fivefold lower counts were identified in the celastrol-treated MCF-7 cells. According to the GO and KEGG analyses, the effects of celastrol on MCF-7 cells forced lipid metabolism and the endocrine system. Moreover, leptin treatment induced phosphorylation of leptin receptor and PI3K/AKT in MCF-7 cells, whereas pretreatment with celastrol partly abrogated leptin activation. The binding of celastrol to the leptin receptor was also confirmed by molecular docking. The antitumor effect of celastrol is proposed to be mediated by its binding to the leptin receptor and controlled down-regulation of the PI3K/AKT pathway.

1. Introduction

Breast cancer (BC), as the malignant tumor with the highest incidence in women in the world, is characterized by rapid progression, easy metastasis and drug resistance. It accounts for 15% of all kinds of cancer deaths globally [1]. Obesity is closely associated with an increased risk of breast cancer in epidemiological studies [2]. However, the molecular mechanisms that link obesity and BC are complex, and leptin signaling has been shown to be an important mediator that promotes tumor proliferation, invasion, migration, and angiogenesis [3]. Leptin and leptin receptors have been regarded as potential targets for novel therapeutic strategies for breast cancer treatment.

The breast is a peculiar organ where epithelial cells are submerged in a fatty environment. The patient outcome of BC has been connected to the activation of lipid metabolism in cancer cells [4].

Leptin is a kind of adipokine that is produced by adipocytes. High levels of leptin are correlated with growth and migration coupled with infiltration of breast tumor cells. The stimulatory influences triggered by leptin were verified in models of nude mice propagated with a breast cancer cell line, where inoculation of leptin remarkably elevated tumor growth [5,6]. Leptin can stimulate angiogenesis via activation of the expression of VEGF (vascular endothelial growth factor). The mRNA and protein expression of the leptin receptor (ObR) have been analyzed in diverse breast cancer cell lines, including MDA-MB-231, MCF-7 and T47D cells [7]. The binding of leptin to ObR leads to the activation of numerous downstream signaling cascades, such as the JAK/STAT3 and PI3K/AKT cascades. The PI3K/AKT signaling pathway is a critical regulatory component in carcinogenesis in breast cancer related to leptin [8]. The activation of JAK2 results in the activation of PI3K/AKT, and PI3K simultaneously activates mTOR [9]. Leptin also enhances the proliferation of BC cells via the PI3K/AKT/SREBP2 signaling pathway [10]. Moreover, AKT phosphorylates and activates endothelial nitric oxide synthase (eNOS), and the PI3K/AKT/eNOS signaling pathway is able to stimulate endothelial cell migration [11]. Collec-

* Corresponding authors at: Hebei University of Chinese Medicine, Shijiazhuang, Hebei 050200, China (F. Liu and Y. Gao).
E-mail addresses: liufei@hebcm.edu.cn (F. Liu), gyg3177@163.com (Y. Gao).

tively, leptin positively regulates PI3K/AKT signaling pathways and promotes cancer growth and angiogenesis of breast cancer. Leptin-targeting drugs may decrease breast cancer risk, improve the clinical outcomes of patients, and control other comorbidities.

Celastrol is a major active component extracted from *Tripterygium wilfordii* (TW), a TCM (traditional Chinese medicinal herb). It has been documented that celastrol harbors curative properties in treating various cancers, such as breast, prostate, ovarian and gastric cancers [12,13]. The anticancer properties of celastrol can be ascribed to different molecular targets, including apoptosis, angiogenesis, cell invasion and metastasis. Celastrol inhibits tumor growth in mice inoculated with human prostate cancer cells by inhibiting AKT/mTOR signaling [14]. It has been reported that celastrol induces apoptosis in human triple-negative breast cancer cells, and its anticancer effect might be mediated through the PI3K/Akt signaling pathway [15].

Notably, recent studies have shown that celastrol acts as a leptin sensitizer and induces a reduction in body fat and leptin levels, whereas this effect is not exhibited in leptin-deficient (ob/ob) or db/db mice, which proves that celastrol regulates leptin signaling [16,17]. Although the effect of celastrol on leptin has already been established, the role of celastrol in leptin-induced proliferation and migration in breast cancer cells is not clear. The link between celastrol and leptin and between leptin and the PI3K/Akt signaling pathway in breast cancer treatment might be a more complex network. In this case, we explored whether the anticancer properties of celastrol may be displayed through the modulation of the leptin axis and, if so, by what mechanism. Here, the effect of celastrol in breast cancer cells (MCF-7) was tested, and the responsible mechanisms were elucidated by transcriptomic analysis and western blotting.

2. Materials and methods

2.1. Agents

Celastrol was obtained from Dalian Meilun Biotechnology Co., Ltd., China, and the celastrol structure is given in Fig. 1. Leptin (cat number: CSN21705) was obtained from CSN.

AKT Mouse Monoclonal Antibody (cat number: 10176-2-AP) and LEPR Antibody (cat number: 20996-1-AP) were obtained from Proteintech, Phospho-AKT (Ser473) Antibody (cat number: 9271), PI3 Kinase p85 Antibody (cat number: 4257), mTOR Antibody (cat number: 2983), Phospho-mTOR (Ser2481) Antibody (cat number: 2974) was obtained from Cell Signaling Technology, Phospho-PI3 Kinase p85 alpha (Tyr607) Antibody (cat number: AF −3241) was obtained from Affinity Biosciences.

2.2. CCK8 assay [18]

MCF-7 cells were inoculated in 96-well plates for 24 h at 37 °C, 5% CO_2 and saturated humidity. A cell counting kit assay was
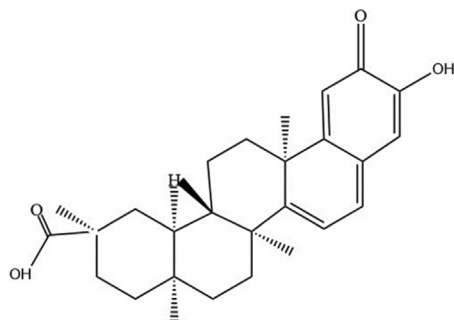
conducted to assess the effect of celastrol on MCF-7 cells. Briefly, MCF-7 cells were inoculated with control culture and various levels (1 μM, 10 μM, 25 μM, 50 μM, 100 μM) of celastrol for 24, 48, and 72 h. Then, after the culture was discarded, 10 μL CCK8 was added to 100 μL of medium for four hours of incubation. Thereafter, the optical density (OD) values were determined on a spectrophotometer at 450 nm.

2.3. Transcriptome sequencing [19]

2.3.1. The protocol of RNA-Seq

After being inoculated with 1 μM celastrol for 48 h, we rinsed the cells with PBS. Then, total RNA (tRNA) was isolated using TRIzol reagent as documented by the manufacturer (Invitrogen). Afterward, the quality and integrity of the tRNA were determined with an Agilent 2100 Bioanalyzer (Agilent Technologies, United States) and run on an agarose gel (1.2%) via electrophoresis. In addition, tRNA quantitation was performed on the NanoDrop 2000 platform (NanoDrop Technologies, Wilmington, DE). Thus, we selected tRNA samples of high quality, i.e., OD260/280 of between 1.8 and 2.2 along with OD260/230 ≥ 2.0 with an RIN (RNA integrity number) ≥ 8, as well as tRNA quantity ≥ 50 ng/μL for processing of RNA libraries.

The Illumina TruSeq™ RNA sample processing kit was adopted to process libraries for RNA sequencing (Illumina, San Diego, CA). In brief, enrichment of mRNAs harboring poly A tails was performed using oligo (dT) magnetic beads from the tRNA. After that, the mRNAs were fragmented with fragmentation buffer into 300-bp fragments. Thereafter, the mRNA fragments were converted into double strand cDNA with the SuperScript ds-cDNA synthesis kit (Invitrogen, CA) as described by the manufacturer. Next, end repair along with A-tailing were performed on the ds-cDNA. We ligated adapter indices onto the ds-cDNA, and then the ds-cDNA was cleaned, followed by enrichment via PCR. The quantity of the ds-cDNA was checked on the TBS380 and NanoDrop 2000 spectrophotometers, while its quality was assessed on the Agilent 2100 Bioanalyzer. Afterward, the processed libraries were utilized for paired-end (PE) sequencing on the Illumina NovaSeq 6000 platform. Merging of the paired-end reads was performed with SeqPrep (https://github.com/jstjohn/SeqPrep) and Sickle (https://github.com/najoshi/sickle). Trimming of the adapters along with the primers was performed, and sequences that were 20 bp long or less were discarded. Afterward, trimming of low-quality at the 3′ ends was performed, and sequences with quality values of 10 or less were discarded. Moreover, reads with N ratios >10% were discarded. Thereafter, we evaluated the error rate (%), Q20 and Q30 values, GC content (%), and sequence duplication levels of the obtained high-quality clean reads.

2.3.2. The high-quality reads were mapped to the reference

Mapping of the high-quality reads was performed to the reference *Bos taurus* genome (UMD3.1) (https://www.ensembl.org/Homo_sapiens/Info/Index) via HISAT2 (https://ccb.jhu.edu/software/hisat2/index.shtml), and the reference-based assembly of transcripts was performed with StringTie (https://ccb.jhu.edu/software/stringtie/). By comparison with the reference *homo sapiens* genome, on the one hand, genes harboring annotation data can be determined in the assembled genome. In addition, transcripts lacking annotated data can be determined and defined as novel transcripts. The prediction of new transcripts was performed with gffcompare software. Thereafter, we employed gene prediction to compute the values of gene expression.

2.3.3. Differential expression analysis

We adopted featureCounts software to compute the read counts of every transcript or gene. The values of gene expression were given in the form of reads per kilobase of exon per million frag-

Fig. 1. The structure of celastrol.

ments mapped (FPKM) via featureCounts software. We employed the FDR (false discovery rate) in rectifying the p values to determine the DEGs (differentially expressed genes). We computed the FC (fold change) of every transcript or gene in the diverse groups. An FDR ≤ 0.05 along with $|Log2FC| \geq 1$ signified statistically significant DEGs. The differential expression assessment of genes or transcripts was performed with DESeq2.

Enrichment analyses of the DEGs were performed via GO and KEGG pathway analyses. In the enrichment assessments, we adopted Fisher's exact test along with a multiple correction approach, consisting of Bonferroni, Sidak, and Holm, as well as the false discovery rate in correcting for the p values along with the false-positive rate. GOatools was employed to perform functional enrichment assessment. $P \leq 0.05$ signified statistically significant GO terms. KOBAS software was employed to perform KEGG pathway enrichment analyses, with $P \leq 0.05$ signifying statistical significance.

2.4. Wound healing assay [20]

We used a wound healing assay to detect the effect of celastrol and leptin on the migration of MCF-7 cells. MCF-7 cells (1.0×10^5) were inoculated in 24-well plates and incubated overnight to attain monolayer confluence. Thereafter, a wound midline scratch was made with a 10 μL pipette tip, and PBS was utilized to rinse the cells twice. This assay was used for two sections. The first section was used to detect the effect of celastrol on the migration of MCF-7 cells. MCF-7 cells were divided into four groups as follows: MCF-7 cells were inoculated with control medium, and MCF-7 cells were inoculated with medium enriched with 0.1, 1, or 10 μM celastrol (these concentrations of celastrol were based on the results of CCK8). The second section was used to detect the effect of celastrol and leptin on the migration of MCF-7 cells. MCF-7 cells were divided into four groups as following: the MCF-7 cells had been inoculated with the control medium, the MCF-7 cells had been inoculated with the medium enriched with 1 μM celastorl alone, the MCF-7 cells had been inoculated with the medium enriched with 100 μg/ml leptin alone, and the MCF-7 cells had been coinoculated with the medium enriched with 1 μM celastorl and 100 μg/ml leptin. After forty-eight hours of culture in RPMI 1640 enriched with two percent serum (control) or stimulation with celastrol and/or leptin, we assessed cell migration by determining the difference in wound area with a Motic Digital Medical Image Analysis Platform (Leica DM2500, Germany) at 0 h and 48 h.

2.5. Transwell chamber migration assay [21]

In this assay, the sections and groups were the same as those in the wound healing assay. MCF-7 cells (2×10^4) that had been inoculated for forty-eight hours were introduced to the Transwell chamber (Corning, United States). We introduced serum into the bottom wells of the compartments to trigger cell migration. After forty-eight hours, the cells that migrated via the membrane were stained with 0.5% methylrosaniline chloride solution and counted. Counting of the cells was performed in five random fields and given as 1% of the average cell numbers per field under a light microscope.

2.6. Autodocking [22]

The interaction between LEPR and celastrol was checked via molecular docking technology. The structures of LEPR were abstracted from the PDB data resource (https://www.rcsb.org/), and the 3D structures of celastrol were drawn by Chemoffice 2017. Molecular docking along with conformation scoring were performed in AutoDock Vina. The structure of the best docking results was drawn by PyMOL and Discovery Studio 2016 Client.

2.7. Western blot [23]

In this assay, the MCF-7 cells were divided into four groups as following: the MCF-7 cells had been inoculated with the control medium, the MCF-7 cells had been inoculated with the medium enriched with 1 μM celastorl alone, the MCF-7 cells had been inoculated with the medium enriched with 100 μg/ml leptin alone, and the MCF-7 cells had been coinoculated with the medium enriched with 1 μM celastorl and 100 μg/ml leptin. After being inoculated for 48 h, the cells were rinsed twice with PBS. The lysis buffer was obtained from Beijing Zomen Biotechnology Co., Ltd. Separation of membrane proteins was performed by ultraspinning. The protein lysates were incubated for five minutes at 5000 rpm at 4 °C. Thereafter, the supernatant was incubated for one hour at 100,000g. The pellet containing the fraction of the crude membrane was resuspended in lysis buffer enriched with 0.2% Triton-100. We introduced the proteins into the loading buffer (Beijing Zomen Biotechnology Co., Ltd.), heat denatured at 95 ℃ for 15 min and subjected to SDS–PAGE (Beijing Zomen Biotechnology Co., Ltd.). The protein contents in cell lysates were quantified with an ND-1000 Spectrophotometer (NanoDrop, USA). Thereafter, fractionation of the proteins was performed on an 8% SDS–PAGE gel and then transferred onto PVDF membranes (Millipore, Billerica, MA) in transfer buffer (Beijing Zomen Biotechnology Co., Ltd.) for three hours at 100 V and inoculated overnight with primary antibody (1:500) at 4 °C or for one hour at RT. Nonspecific docking was blocked by using 1.5% (w/v) evaporated skimmed milk (Difco, USA) in TBST (Beijing Zomen Biotechnology Co., Ltd.). Afterward, the membranes were inoculated with anti-rabbit or anti-mouse secondary antibodies linked to IRDye700DX and IRDye800CW (1:5000; Rockland, USA). Detection and quantification were performed on the Odyssey imaging platform of LI-COR Biosciences in the USA. Equal amounts of heat-denatured proteins were fractionated on an SDS–PAGE gel and probed onto PVDF membranes (Millipore, USA). Afterward, blocking of the membranes was performed in 5% milk in the room for two hours and overnight inoculated with primary antibodies at 4 ℃ and with secondary antibodies for two hours at 37 ℃.

2.8. Statistical analysis

SPSS 26.0 statistical software package was used for data analysis. The normal distribution of data was tested by the Shapiro-Wilk test. Continuous data with a normal distribution are given as the mean ± standard deviation (SD) for the specified number of independent experiments. Means of the continuous normal distribution variables were compared via one-way analysis of variance (ANOVA) coupled with the Tukey HSD post hoc test. P <.05 signified statistical significance.

3. Results

3.1. Celastrol dampened the proliferation of MCF-7 cells

Celastrol dampened the growth of MCF-7 cells in a concentration- and time-dependent manner, as shown in Fig. 2. Analyzing the results of the CCK-8 assay, the IC_{50} values of celastrol against MCF-7 cells after 24, 48, and 72 h were 22.68 ± 1.46 μM, 7.56 ± 0.89 μM and 0.89 ± 0.067 μM, respectively.

3.2. The effects of celastrol on the mRNA expression of MCF-7 cells

Given the results of the CCK-8 assay, we wondered about the molecular mechanisms by which celastrol dampened the proliferation of MCF-7 cells. Therefore, we assessed patterns of alterations in the transcriptome via RNA sequencing (RNA-Seq) of mRNA har-
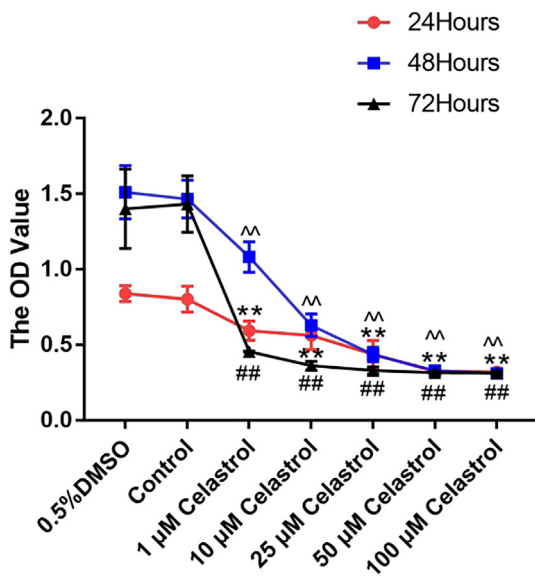
Fig. 2. The effect of celastrol on the growth of MCF-7 cells.

26,414 mRNAs were obtained from control and celastrol-treated samples, and the results are shown as MA plots and volcano plots (Fig. 3-A). We identified 2033 mRNAs with twofold higher counts ('upregulated') and 1898 mRNAs with twofold lower counts ('downregulated') in celastrol-inoculated samples vs. controls. Furthermore, 52 mRNAs had fivefold higher counts ('upregulated') and 149 mRNAs had fivefold lower counts ('downregulated') in celastrol-treated samples vs. controls (Fig. 3-B). According to the GO and KEGG analyses for all identical genes (Fig. 3-C and D), the effects of celastrol on MCF-7 cells were forced on cellular processes, lipid metabolism and the endocrine system.

3.3. Celastrol dampened the migration of MCF-7 cells

The exposure of MCF-7 cells to celastrol caused a concentration-dependent dampening of migration (Fig. 4). As shown in Fig. 4, leptin enhanced the migration of MCF-7 cells, while celastrol dampened the effects of leptin on the migration of MCF-7 cells.

3.4. The relationship of celastrol and long leptin receptor (LEPR)

Celastrol docked with the protein structures of LEPR. The results showed that celastrol has good docking potential to LEPR, and the Vina score (ΔG) was -6.60 kca1/mol. Molecular docking revealed the celastrol bond with LEPR through hydrophobic interactions and electrostatic interactions at sites such as TRP872, LEU870, and ASP874 (Fig. 5).
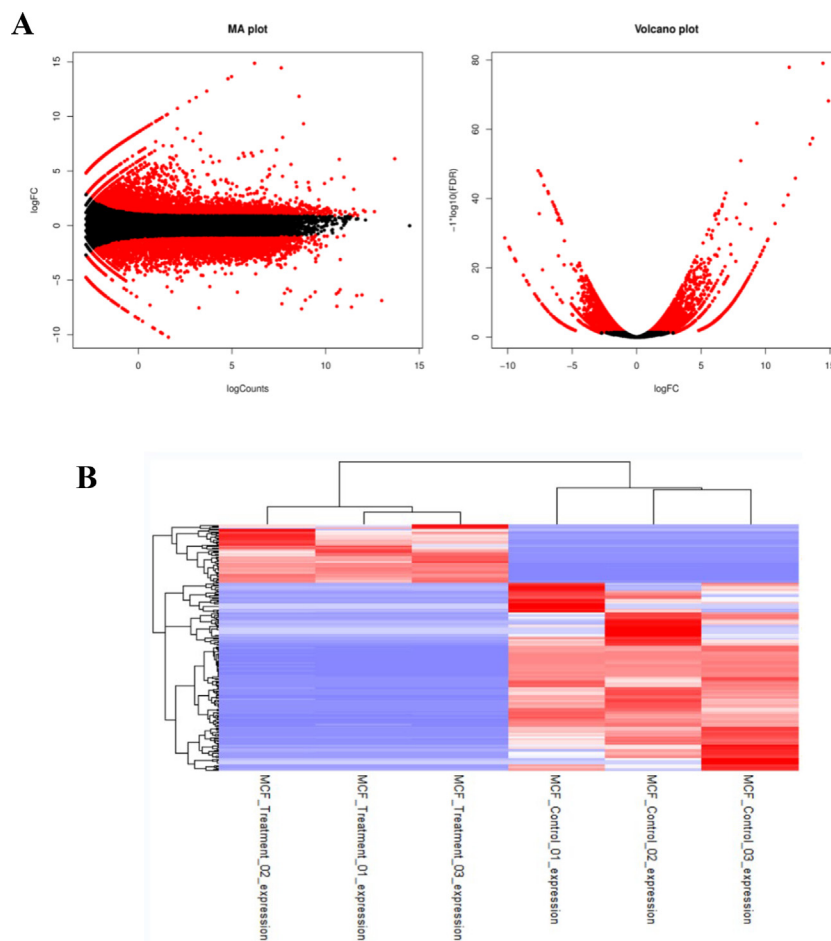
vested from MCF-7 cells treated for 48 h with 1 μM celastrol. Six independent biological replicates were employed for transcriptome sequencing. After data processing and averaging of replicates,

Fig. 3. The impacts of celastrol on the mRNA expression of MCF-7 cells. A: MA plot and volcano plot of 26,414 mRNAs from control and celastrol-treated samples. B: Heatmap of up/downregulated unigenes (fivefold more counts) in control and celastrol-treated samples.. C: GO analysis of up/downregulated unigenes in control and celastrol-treated samples. D: KEGG analysis of up/downregulated unigenes in control and celastrol-treated samples.
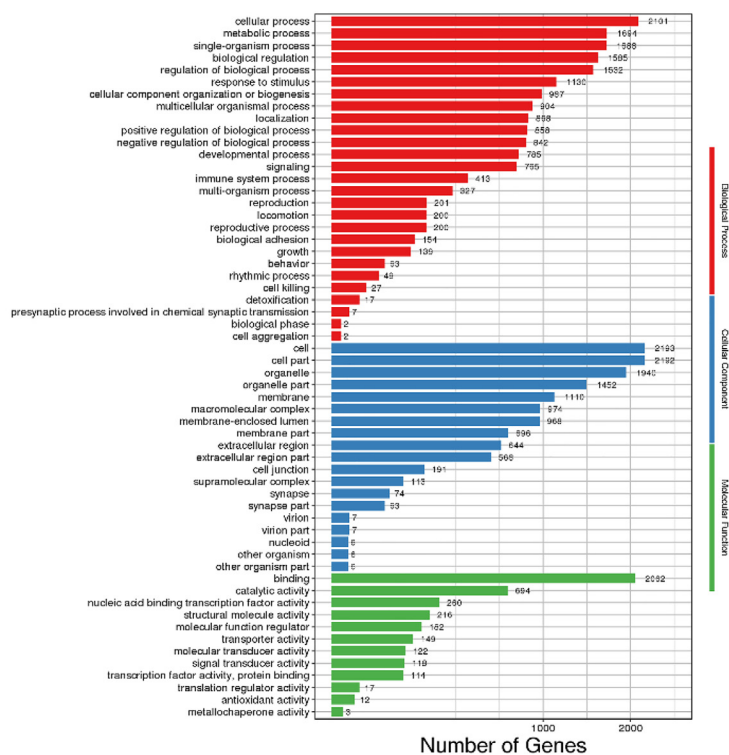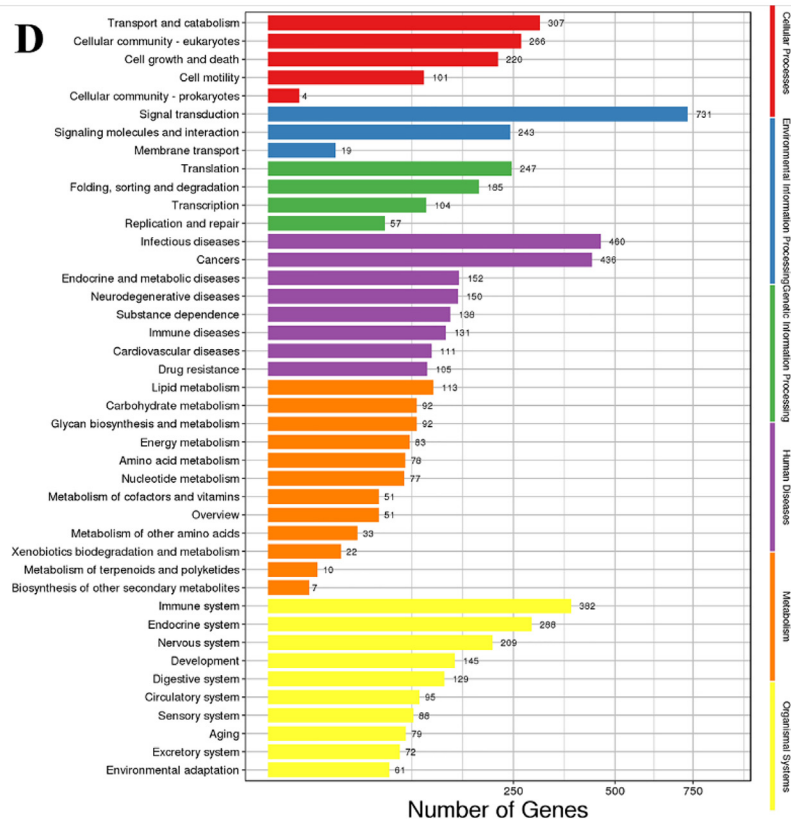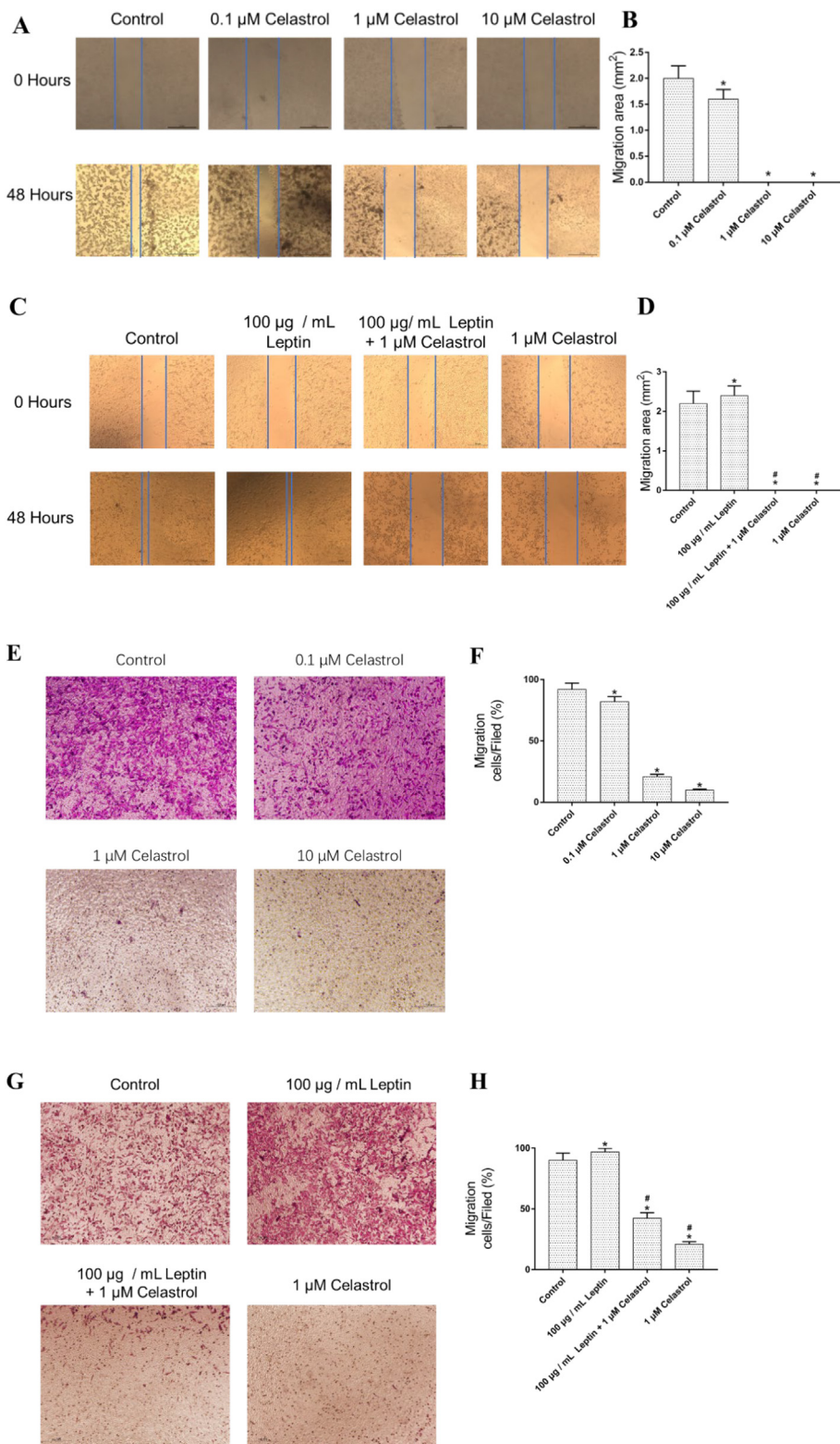
Fig. 3 (*continued*)

Fig. 4. Effects of celastrol and leptin on the migration of MCF-7 cells. A: Typical photos of the impact of celastrorl on the migration of MCF-7 cells using a wound healing assay. B: Statistical analysis of the influence of celastrol on the migration area (mm^2) of MCF-7 cells. *P <.05 *in contrast with the* control. C: Typical figures of the wound-healing assay for the impact of celastrorl on the leptin-stimulated migration of MCF-7 cells. D: Statistical analysis of the effect of celastrorl and leptin on the migration area (mm^2) of MCF-7 cells. *P <.05 *vs.* control, #P <.05 *relative to* leptin (n = 3). E: Typical photos of the effect of celastrorl on the migration of MCF-7 cells via the Transwell chamber migration assay. F: Statistical analysis of the impact of celastrorl on the ratio of migrating MCF-7 cells to filled MCF-7 cells (%). *P <.05 *in contrast with the* control. G: Typical figures of the transwell chamber migration assay for the effect of celastrorl on leptin-stimulated MCF-7-cell migration. H: Statistical analysis of the effect of celastrorl and leptin on the ratio of migrating MCF-7 cells to filled MCF-7 cells (%). *P <.05 relative to the control, #P <.05 *in contrast with* leptin (n = 3).
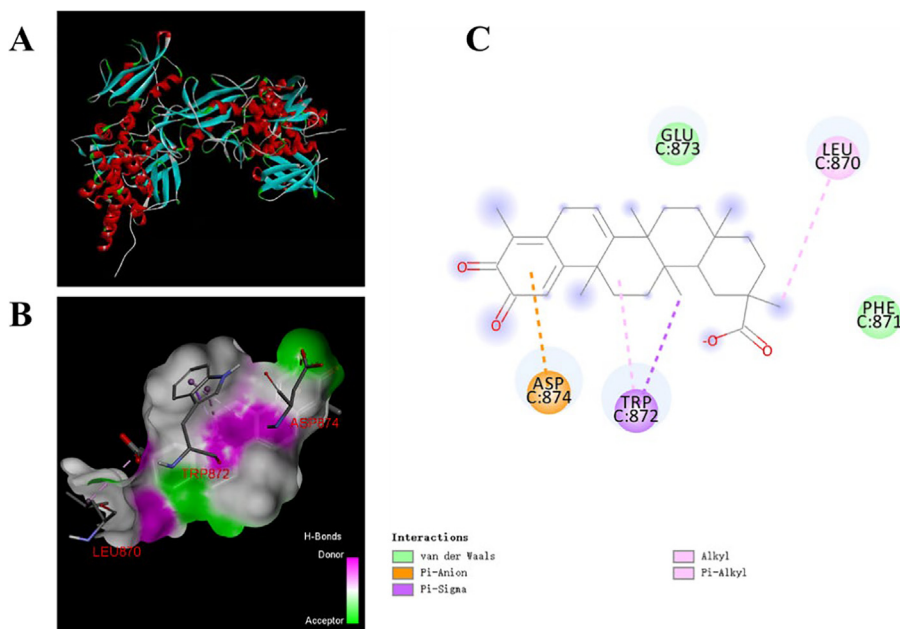
Fig. 5. Results of molecular docking of celastrol and LEPR. A: The 3D structure of LEPR. B: 3D Diagram of crosstalk between celastrol and LEPR. C: 2D Diagram of cross talk between celastrol and LEPR.
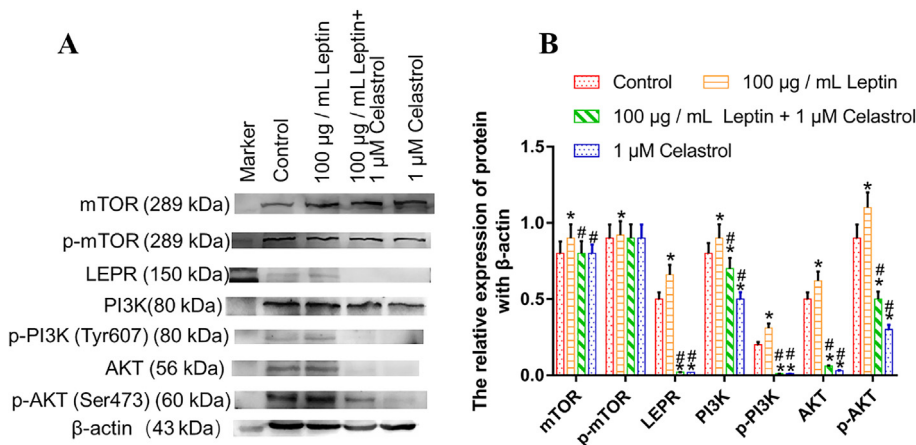

Fig. 6. The impacts of celastrol and leptin on PI3K, LEPR, p-PI3K, p-mTOR, AKT, and p-PI3K mTOR expression in MCF-7 cells. A: The typical results of the effects of celastrol and leptin on PI3K, p-PI3K mTOR, p-PI3K, LEPR, AKT, and p-mTOR expression in MCF-7 cells via Western blot. B: Statistical analysis of the effects of celastrol and leptin on PI3K, p-PI3K mTOR, AKT, p-mTOR, p-PI3K, and LEPR expression in MCF-7 cells via Western blot. *P <.05 in contrast with the control, #P <.05 relative to leptin (n = 3).

3.5. The effects of celastrol and leptin on PI3K, AKT, mTOR and LEPR expression in MCF-7 cells

Celastrol dampened the expression of PI3, p-PI3K, AKT, p-PI3K and LEPR (Fig. 6). As shown in Fig. 6, leptin enhanced the expression of PI3K, AKT, p-PI3K, p-PI3K mTOR, p-mTOR and LEPR in MCF-7 cells, while celastrol dampened the effects of leptin on the expression of PI3K, LEPR, p-PI3K, AKT, and p-PI3K in MCF-7 cells.

4. Discussion

Leptin, a product of the obese (Ob) gene, influences appetite control, angiogenesis, energy balance along with the proliferation of diverse cell types, including breast cells [24]. Under conditions of obesity, a high level of leptin binds to ObR expressed in BC cells to affect various steps of breast tumor progression. Evidence from clinical and experimental studies supports that leptin is a remarkable molecular mediator of the obesity-breast cancer axis

[25,26]. Drugs targeting leptin signaling may diminish breast cancer risk and improve clinical outcomes. Celastrol, a promising anticancer drug extracted from traditional Chinese medicinal herbs, has recently emerged as a candidate to treat obesity by improving leptin sensitivity [27,28]. Here, the growth coupled with the migration of breast cancer cells (MCF-7) induced by leptin was tested to demonstrate the antineoplastic activity of celastrol. Transcriptomic analysis and western blotting were conducted to explore the biological roles of leptin in treating BC with celastrol.

First, a CCK-8 assay was used to detect the effect of celastrol on the proliferation of MCF-7 cells. The median inhibition concentration (IC$_{50}$) of celastrol to MCF-7 cells for 72 h was lower than that for 48 h, and that for 48 h was lower than that for 48 h, as illustrated via CCK-8 assay. Celastrol suppressed the growth of MCF-7 cells in a concentration- and time-dependent manner. Similar results were reported by another group using MDA-MB-231, as well as triple–negative breast cancer (TNBC) cells [29,30].

Given the results of the CCK-8 assay, we wondered about the molecular mechanisms by which celastrol dampened the proliferation of MCF-7 cells, especially the biological roles of leptin in the process. Therefore, we assessed patterns of transcriptome changes in MCF-7 cells inoculated with celastrol. High-throughput RNA sequencing is widely used for studying transcriptomes. RNA-seq combines molecular biology approaches for RNA amplification with bioinformatics tools for measuring and validating large RNA-seq datasets [31]. According to the GO and KEGG analyses for all identical genes in our study, the molecular mechanisms of celastrol in MCF-7 cells could block cellular processes and lipid metabolism and disturb the endocrine system. Other studies have shown that celastrol has the ability to regulate leptin sensitivity, energy metabolism and lipid metabolism [32]. Combined with our RNA-seq results, the anticancer effects of celastrol on MCF-7 cells could be forced on lipid metabolism and the endocrine system.

Indeed, the relationship between obesity, lipid metabolism and leptin seems to be a complex signaling transduction network that regulates diverse aspects of breast cancer biology from primary tumor growth to the formation of metastases [33]. Importantly, leptin is regarded as a remarkable molecular mediator in this signaling network [25,26]. The present findings in our study showed that celastrol at a concentration of 1 μM remarkably reversed leptin-triggered migration in MCF-7 cells in the wound healing assay and transwell chamber migration assay, and the binding of celastrol to the leptin receptor was also confirmed by molecular docking. Notably, leptin receptor phosphorylation was also reversed by celastrol in breast cancer cells in the present work. Previous investigations have reported that the antiobesity effect of celastrol largely depends on leptin receptor signaling [34]. As a key modulator in the development of obesity along with breast cancer, leptin is able to stimulate the proliferation of malignant breast epithelial cells through several signaling cascades, such as PI3K/AKT, JAK2/STAT3 and MAPK [11]. Additionally, our data show that leptin treatment induced phosphorylation of the leptin receptor and PI3K/AKT in MCF-7 cells, whereas pretreatment with celastrol partly abrogated leptin activation. PI3K belongs to the lipid kinase family and is involved in both the development of cancer and obesity [35]. AKT is an important downstream target of PI3K, which is closely related to tumor development. The PI3K/AKT/mTOR cascade is linked to numerous characteristics of cancer, such as the cell cycle, growth and motility [36,37]. Therefore, we conclude that the antitumor effect of celastrol is mediated by its binding to ObR, which therefore inhibits the impact of PI3K/AKT on breast cancer. In particular, leptin also amplifies estrogen signaling, which contributes to breast tumorigenesis [33,38]. Leptin receptor isoforms and estrogen receptor-α were jointly expressed in breast cancer cell lines [39]. These data support the KEGG pathway analysis in our study, which suggested that estrogen signaling pathways may be connected with celastrol acting on breast cancer. According to the western blot results, celastrol dampened the expression of PI3K, p-PI3K, AKT, p-PI3K and LEPR, and leptin enhanced the expression of PI3K, AKT, p-PI3K, p-PI3K mTOR, p-mTOR and LEPR in MCF-7 cells, while celastrol dampened the effects of leptin on the expression of PI3K, LEPR, p-PI3K, AKT, along with p-PI3K in MCF-7 cells, so celastrol reversed the leptin-triggered PI3K/AKT/mTOR pathway in breast cancer.

The effect of celastrol in breast cancer is extensive and significant. Leptin is responsible in part for the effects of celastrol in controlling the PI3K/AKT pathway, thereby resulting in decreased proliferation of MCF-7 cells. However, the upstream regulators and downstream effectors of leptin-PI3K/AKT have not yet been fully explained. Further studies may be conducted to provide profound insight into the anticancer mechanism of celastrol, especially the role of leptin in cancer therapies in the obese environment.

5. Conclusion

Celastrol reversed leptin-triggered cell proliferation and migration in MCF-7 cells in a concentration- and time-dependent manner. According to the transcriptome changes for all identical genes of MCF-7 cells inoculated with celastrol, the effects of celastrol on MCF-7 cells were forced on cellular processes, lipid metabolism and the endocrine system. Celastrol has good docking potential to the long leptin receptor. Moreover, leptin treatment induced phosphorylation of PI3K/AKT/mTOR in MCF-7 cells, whereas pretreatment with celastrol partly abrogated leptin activation. The antitumor effect of celastrol is proposed to be mediated by its binding to the leptin receptor and controlled downregulation of the PI3K/AKT pathway.

Declaration of Competing Interest

The authors declare that they have no known competing financial interests or personal relationships that could have appeared to influence the work reported in this paper.

Author statement

The conception of the experiment was designed by Fei Liu and Yonggang Gao; Pingping Chen and Bin Wang performed the experiment and collated and analyzed the data; Meng Li and Chunxue Cui critically revised the work.

Compliance with ethical standards

Conflict of interest: None.
Ethical statements: Our work does not use animals or humans, so ethics approval (including appropriate approvals or waivers) is not applicable.

References

[1] Siegel RL, Miller KD, Fuchs HE, Jemal A. Cancer statistics. CA Cancer J Clin 2021;71(1):7–33. https://doi.org/10.3322/caac.21654.

[2] Lee K, Kruper L, Dieli-Conwright CM, Mortimer JE. The impact of obesity on breast cancer diagnosis and treatment. Curr Oncol Rep 2019;21(5):41. https://doi.org/10.1007/s11912-019-0787-1.

[3] García-Estevez L, González-Martínez S, Moreno-Bueno G. The leptin axis and its association with the adaptive immune system in breast cancer. Front Immunol 2021;12:. https://doi.org/10.3389/fimmu.2021.784823784823.

[4] Hoy AJ, Nagarajan SR, Butler LM. Tumour fatty acid metabolism in the context of therapy resistance and obesity. Nat Rev Cancer 2021;21(12):753–66. https://doi.org/10.1038/s41568-021-00388-4.

[5] García-Miranda A, Solano-Alcalá KA, Montes-Alvarado JB, Rosas-Cruz A, Reyes-Leyva J, et al. Autophagy mediates leptin-induced migration and ERK activation in breast cancer cells. Front Cell Dev Biol 2021;9:. https://doi.org/10.3389/fcell.2021.644851644851.

[6] Yuan HJ, Sun KW, Yu K. Leptin promotes the proliferation and migration of human breast cancer through the extracellular-signal regulated kinase pathway. Mol Med Rep 2014;9(1):350–4. https://doi.org/10.3892/mmr.2013.1786.

[7] Hosney M, Sabet S, El-Shinawi M, Gaafar KM, Mohamed MM. Leptin is overexpressed in the tumor microenvironment of obese patients with estrogen receptor positive breast cancer. Exp Ther Med 2017;13(5):2235–46. https://doi.org/10.3892/etm.2017.4291.

[8] Barone I, Giordano C, Bonofiglio D, Andò S, Catalano S. Leptin, obesity and breast cancer: progress to understanding the molecular connections. Curr Opin Pharmacol 2016;31:83–9. https://doi.org/10.1016/j.coph.2016.10.003.

[9] Sánchez-Jiménez F, Pérez-Pérez A, de la Cruz-Merino L, Sánchez-Margalet V. Obesity and breast cancer: role of leptin. Front Oncol 2019;9:596. https://doi.org/10.3389/fonc.2019.00596.

[10] Atoum MF, Alzoughool F, Al-Hourani H. Linkage between obesity leptin and breast cancer. Breast Cancer (Auckl). 2020; 14:1178223419898458. doi: 10.1177/1178223419898458.

[11] Andò S, Catalano S. The multifactorial role of leptin in driving the breast cancer microenvironment. Nat Rev Endocrinol 2011;8(5):263–75. https://doi.org/10.1038/nrendo.2011.184.

[12] Ng SW, Chan Y, Chellappan DK, Madheswaran T, Zeeshan F, et al. Molecular modulators of celastrol as the keystones for its diverse pharmacological activities. Biomed Pharmacother 2019;109:1785–92. https://doi.org/10.1016/j.biopha.2018.11.051.

[13] Li X, Wang H, Ding J, Nie S, Wang L, et al. Celastrol strongly inhibits proliferation, migration and cancer stem cell properties through suppression of Pin1 in ovarian cancer cells. Eur J Pharmacol 2019;842:146–56. https://doi.org/10.1016/j.ejphar.2018.10.043.

[14] Pang X, Yi Z, Zhang J, Lu B, Sung B, et al. Celastrol suppresses angiogenesis-mediated tumor growth through inhibition of AKT/mammalian target of rapamycin pathway. Cancer Res 2010;70(5):1951–9. https://doi.org/10.1158/0008-5472.CAN-09-3201.

[15] Shrivastava S, Jeengar MK, Reddy VS, Reddy GB, Naidu VG. Anticancer effect of celastrol on human triple negative breast cancer: possible involvement of oxidative stress, mitochondrial dysfunction, apoptosis and PI3K/Akt pathways. Exp Mol Pathol 2015;98(3):313–27. https://doi.org/10.1016/j.yexmp.2015.03.031.

[16] Feng X, Guan D, Auen T, Choi JW, Salazar Hernández MA, et al. IL1R1 is required for celastrol's leptin-sensitization and antiobesity effects. Nat Med 2019;25(4):575–82. https://doi.org/10.1038/s41591-019-0358-x.

[17] Xu S, Feng Y, He W, Xu W, Xu W, et al. Celastrol in metabolic diseases: Progress and application prospects. Pharmacol Res 2021;167:. https://doi.org/10.1016/j.phrs.2021.105572105572.

[18] Hammond C, Paupardin-Tritsch D, Nairn AC, Greengard P, Gerschenfeld HM. Cholecystokinin induces a decrease in Ca2+ current in snail neurons that appears to be mediated by protein kinase C. Nature 1987;325(6107):809–11. https://doi.org/10.1038/325809a0. PMID: 2434859.

[19] Welleford AS, Quintero JE, Seblani NE, Blalock E, Gunewardena S, et al. RNA sequencing of human peripheral nerve in response to injury: distinctive analysis of the nerve repair pathways. Cell Transplant 2020; 29:963689720926157. doi: 10.1177/0963689720926157.

[20] Lewis H, Lance R, Troyer D, Beydoun H, Hadley M, et al. miR-888 is an expressed prostatic secretions-derived microRNA that promotes prostate cell growth and migration. Cell Cycle 2014;13(2):227–39. https://doi.org/10.4161/cc.26984.

[21] Zhu G, Cheng Z, Huang Y, Zheng W, Yang S, et al. MyD88 mediates colorectal cancer cell proliferation, migration and invasion via NF-κB/AP-1 signaling pathway. Int J Mol Med 2020;45(1):131–40. https://doi.org/10.3892/ijmm.2019.4390.

[22] Sun B, Luo C, Zhang X, Guo M, Sun M, et al. Probing the impact of sulfur/selenium/carbon linkages on prodrug nanoassemblies for cancer therapy. Nat Commun 2019;10(1):3211. https://doi.org/10.1038/s41467-019-11193-x.

[23] Avtanski D, Garcia A, Caraballo B, Thangeswaran P, Marin S, et al. In vitro effects of resistin on epithelial to mesenchymal transition (EMT) in MCF-7 and MDA-MB-231 breast cancer cells - qRT-PCR and Westen blot analyses data. Data Brief 2019;25:. https://doi.org/10.1016/j.dib.2019.104118104118.

[24] Andò S, Barone I, Giordano C, Bonofiglio D, Catalano S. The multifaceted mechanism of leptin signaling within tumor microenvironment in driving breast cancer growth and progression. Front Oncol 2014;4:340. https://doi.org/10.3389/fonc.2014.00340.

[25] Rock CL, Pande C, Flatt SW, Ying C, Pakiz B, et al. Favorable changes in serum estrogens and other biologic factors after weight loss in breast cancer survivors who are overweight or obese. Clin Breast Cancer 2013;13(3):188–95. https://doi.org/10.1016/j.clbc.2012.12.002.

[26] Kim J, Jung E, Choi J, Min DY, Lee YH, et al. Leptin is a direct transcriptional target of EGR1 in human breast cancer cells. Mol Biol Rep 2019;46(1):317–24. https://doi.org/10.1007/s11033-018-4474-3.

[27] Liu J, Lee J, Salazar Hernandez MA, Mazitschek R, Ozcan U. Treatment of obesity with celastrol. Cell 2015;161(5):999–1011. https://doi.org/10.1016/j.cell.2015.05.011.

[28] Hu W, Wang L, Du G, Guan Q, Dong T, et al. Effects of microbiota on the treatment of obesity with the natural product celastrol in rats. Diabetes Metab J 2020;44(5):747–63. https://doi.org/10.4093/dmj.2019.0124.

[29] You D, Jeong Y, Yoon SY, A Kim S, Kim SW, et al. Celastrol attenuates the inflammatory response by inhibiting IL 1β expression in triple negative breast cancer cells. Oncol Rep. 2021;45(6):89. doi: 10.3892/or.2021.8040.

[30] Ramamoorthy P, Dandawate P, Jensen RA, Anant S. Celastrol and triptolide suppress stemness in triple negative breast cancer: notch as a therapeutic target for stem cells. Biomedicines 2021;9(5):482. https://doi.org/10.3390/biomedicines9050482.

[31] Babarinde IA, Li Y, Hutchins AP. Computational methods for mapping, assembly and quantification for coding and non-coding transcripts. Comput Struct Biotechnol J 2019;17:628–37. https://doi.org/10.1016/j.csbj.2019.04.012.

[32] Yang X, Wu F, Li L, Lynch EC, Xie L, et al. Celastrol alleviates metabolic disturbance in high-fat diet-induced obese mice through increasing energy expenditure by ameliorating metabolic inflammation. Phytother Res 2021;35(1):297–310. https://doi.org/10.1002/ptr.6800.

[33] Andò S, Gelsomino L, Panza S, Giordano C, Bonofiglio D, et al. Obesity, leptin and breast cancer: epidemiological evidence and proposed mechanisms. Cancers (Basel) 2019;11(1):62. https://doi.org/10.3390/cancers11010062.

[34] Saito K, Davis KC, Morgan DA, Toth BA, Jiang J, et al. Celastrol reduces obesity in MC4R deficiency and stimulates sympathetic nerve activity affecting metabolic and cardiovascular functions. Diabetes 2019;68(6):1210–20. https://doi.org/10.2337/db18-1167.

[35] Klil-Drori AJ, Azoulay L, Pollak MN. Cancer, obesity, diabetes, and antidiabetic drugs: is the fog clearing? Nat Rev Clin Oncol 2017;14(2):85–99. https://doi.org/10.1038/nrclinonc.2016.120.

[36] Le Rhun E, Bertrand N, Dumont A, Tresch E, Le Deley MC, et al. Identification of single nucleotide polymorphisms of the PI3K-AKT-mTOR pathway as a risk factor of central nervous system metastasis in metastatic breast cancer. Eur J Cancer 2017;87:189–98. https://doi.org/10.1016/j.ejca.2017.10.006.

[37] O'Donnell JS, Massi D, Teng MWL, Mandala M. PI3K-AKT-mTOR inhibition in cancer immunotherapy, redux. Semin Cancer Biol 2018;48:91–103. https://doi.org/10.1016/j.semcancer.2017.04.015.

[38] Binai NA, Damert A, Carra G, Steckelbroeck S, Löwer J, et al. Expression of estrogen receptor alpha increases leptin-induced STAT3 activity in breast cancer cells. Int J Cancer 2010;127(1):55–66. https://doi.org/10.1002/ijc.25010.

[39] Raut PK, Choi DY, Kim SH, Hong JT, Kwon TK, et al. Estrogen receptor signaling mediates leptin-induced growth of breast cancer cells via autophagy induction. Oncotarget 2017;8(65):109417–35. https://doi.org/10.18632/oncotarget.22684.